



**A Strategically Managed Rechargeable Battery System with  
a Neutral Methyl Viologen Anolyte and an Acidic Air-Cathode  
Enabled by a Mediator-ion Solid Electrolyte**

Journal:	<i>Sustainable Energy &amp; Fuels</i>
Manuscript ID	SE-COM-05-2018-000227.R1
Article Type:	Communication
Date Submitted by the Author:	27-May-2018
Complete List of Authors:	Yu, Xingwen; University of Texas at Austin, Materials Science and Engineering Manthiram, Arumugam; University of Texas at Austin, Materials Science and Engineering



## Sustainable Energy &amp; Fuels

## COMMUNICATION

## A Strategically Managed Rechargeable Battery System with a Neutral Methyl Viologen Anolyte and an Acidic Air-Cathode Enabled by a Mediator-ion Solid Electrolyte†

Received 00th January 20xx,  
Accepted 00th January 20xx

DOI: 10.1039/x0xx00000x

[www.rsc.org/](http://www.rsc.org/)

Xingwen Yu and Arumugam Manthiram\*

Redox flow batteries with organic electrode materials are attracting much attention. Previous research efforts have been focusing on liquid-phase electrodes on both the anode and cathode sides. Since batteries based on air cathodes can provide immense advantages, coupling a liquid organic electrode with a gaseous air cathode could offer multiple benefits in terms of cost, safety, and energy density. Herein we present a liquid – gaseous battery system with an aqueous methyl viologen (MV) anode and an air cathode. However, under the traditional battery operation principle with the same electrolyte at the anode and cathode, the resulting MV-air battery will not be able to provide a reasonable voltage for practical applications. In this study, the cell voltage of the MV-air chemistry is strategically manipulated by using an acidic cathode electrolyte (catholyte) and a neutral anode electrolyte (anolyte). To operate a battery with different electrolytes at the anode and cathode, a sodium-ion (Na<sup>+</sup>-ion) conductive solid-state electrolyte (Na-SSE) membrane is employed to physically and electrically separate the two electrodes. The shuttling of sodium ions via the Na-SSE balances the ionic charge transfer between the two electrodes and sustains the redox reactions at the air cathode and the MV anode.

### Introduction

Redox flow batteries are considered as a viable electrochemical energy storage technology to efficiently utilize clean energy harvested from renewable resources, such as wind and solar.<sup>1, 2</sup> However, due to a series of challenges, such as crossover of active materials between the two electrodes through the conventional ion-exchange separators leading to a lower efficiency, cost, and chemical toxicity, a widespread implementation of conventional redox flow batteries is still limited.<sup>3-5</sup> To achieve the goal of cost-effective, environmentally benign, safe energy storage systems, recent research in redox flow batteries tending to shift from inorganic electrode materials to organic electrode materials.<sup>6-11</sup> To date, most of the organic redox flow batteries have been developed with liquid-phase electrodes on both the anode and cathode sides.<sup>12-15</sup> Interestingly, electrochemical cells with an air cathode can offer a sequence of technological advantages, such as reducing the volume, weight, and

cost of the battery systems. With the use of free O<sub>2</sub> from the atmosphere, the above technical merits can be easily achieved.<sup>16-21</sup> However, metal-based anodes have been the main focus in the literature to couple with the air cathode to develop metal-air batteries.<sup>22-25</sup> Rechargeable batteries with organic liquid - air chemistries have sparsely been reported.

In this study, we present a new battery chemistry with a liquid-phase organic anode (Methyl viologen, MV) and a gas-phase air cathode. To achieve a practically acceptable cell voltage, the MV-air battery is strategically developed with an acidic cathode electrolyte (catholyte) and a neutral anode electrolyte (anolyte). The catholyte and anolyte with different pH values are physically and electrically separated with a mediator-ion (Na<sup>+</sup>-ion) solid-state electrolyte (Na-SSE) membrane. The Na<sup>+</sup>-ions migrate back and forth through the Na-SSE during charge-discharge, acting as an ionic messenger to maintain the ionic charge balance between the two electrodes.

### Results and Discussion

Methyl viologen (MV), which is *N,N'*-dimethyl-4,4'-bipyridinium dichloride ([C<sub>6</sub>H<sub>7</sub>N]<sub>2</sub>Cl<sub>2</sub>), is an electrochemically active organic material. It has recently been pursued as a liquid-phase electrode material in aqueous solutions.<sup>26, 27</sup> Methyl viologen mainly exists in three oxidation states, MV<sup>0</sup>, MV<sup>+</sup>, and MV<sup>2+</sup>.<sup>28, 29</sup> The transition between MV<sup>2+</sup> and MV<sup>+</sup> as well as that between MV<sup>+</sup> and MV<sup>0</sup> involves one-electron transfer in each process.<sup>30-32</sup> Redox reactions of the methyl viologen species are schematized in Fig. 1a. A cyclic voltammetry (CV) profile of a platinum electrode in a solution containing 0.1 M [C<sub>6</sub>H<sub>7</sub>N]<sub>2</sub>Cl<sub>2</sub> and 0.5 M Na<sub>2</sub>SO<sub>4</sub> (serves as a supporting electrolyte) is presented in Fig. 1b. The two reduction waves at *ca.* -0.52 V and *ca.* -0.95 V correspond, respectively, to the

*Materials Science and Engineering Program & Texas Materials Institute, The University of Texas at Austin, Austin, Texas 78712, USA.*  
Email: [manth@austin.utexas.edu](mailto:manth@austin.utexas.edu).

†Electronic Supplementary Information (ESI) available: Details of experimental methods, a picture and a scanning electron microscopy (SEM) image of a piece of carbon cloth matrix, a picture and a SEM image of a piece of titanium mesh supported iridium oxide (IrO<sub>2</sub>/Ti) catalyst, color change of the anolyte during charging a MV(neutral) || Na-SSE || air (acid) cell, consecutive charge-discharge profiles of the MV (neutral) || Na-SSE || air (acid) cells at different cycling current densities, an SEM image of a carbon cloth matrix after 50 cycles, Figs. S1 – S5. See DOI: 10.1039/x0xx00000x

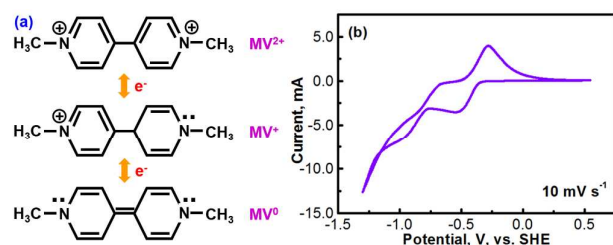


**Fig. 1.** (a) Schematics of the electrochemical reactions of methyl viologen species. (b) A cyclic voltammogram (CV) of a platinum electrode in a 0.1 M methyl viologen + 0.5 M  $\text{Na}_2\text{SO}_4$  solution at a scan rate of  $10 \text{ mV s}^{-1}$ .

reduction of  $MV^{2+}$  to  $MV^+$  and that of  $MV^+$  to  $MV^0$ .<sup>33, 34</sup> For the anodic process, the two oxidation waves at *ca.* -0.66 V and *ca.* -0.27 V correspond, respectively, to the oxidation of  $MV^0$  to  $MV^+$  and that of  $MV^+$  to  $MV^{2+}$ . It can be seen that the first-step redox reaction of  $MV^{2+} \leftrightarrow MV^+$  is highly reversible. However, the reversibility of the second-step reaction of  $MV^+ \leftrightarrow MV^0$  is relatively poor. According to the previous fundamental studies, the transition process of  $MV^+ \leftrightarrow MV^0$  is actually electrochemically reversible.<sup>35</sup> However, the poor reversibility of the  $MV^+ \leftrightarrow MV^0$  couple in aqueous solution, as observed in Fig. 1b, is most likely due to the poor solubility and the uncharged feature of the  $MV^0$  species.<sup>35</sup> Therefore, the electrochemical transition reaction between the  $MV^{2+}$  and the  $MV^+$  species will be an ideal redox couple for the development of redox flow batteries.

Fig. 2 presents the cyclic voltammograms of the redox reaction of  $MV^{2+} \leftrightarrow MV^+$  in 0.1 M  $[(\text{C}_6\text{H}_7\text{N})_2]\text{Cl}_2$  + 0.5 M  $\text{Na}_2\text{SO}_4$  solutions with different pH values. As seen in Fig. 2a, under neutral or alkaline conditions, the transition reaction of  $MV^{2+}/MV^+$  is highly reversible without any significant side reactions. The redox potential of  $MV^{2+}/MV^+$  is almost identical at the pH values of 7 to 13. However, as seen in Fig. 2b, the reversibility of the  $MV^{2+}/MV^+$  reaction is poor under acidic conditions. It is almost irreversible at low pH values. Therefore, the methyl viologen can only be used as an

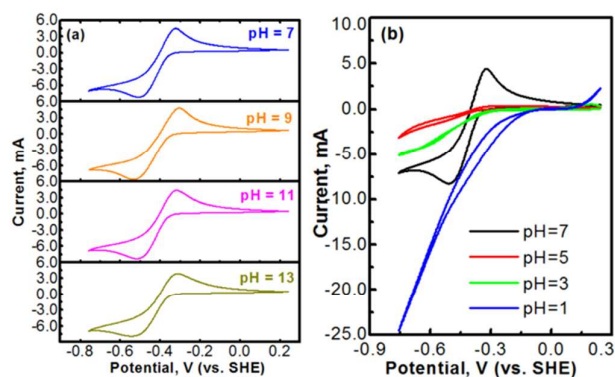
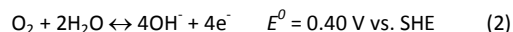


**Fig. 2.** (a) Cyclic voltammograms (CVs) of a platinum electrode in 0.1 M  $[(\text{C}_6\text{H}_7\text{N})_2]\text{Cl}_2$  + 0.5 M  $\text{Na}_2\text{SO}_4$  solutions with different pH values of 7, 9, 11, and 13. (b) CVs of a platinum electrode in 0.1  $[(\text{C}_6\text{H}_7\text{N})_2]\text{Cl}_2$  + 0.5 M  $\text{Na}_2\text{SO}_4$  solutions with different pH values of 7, 5, 3, and 1. The scan rate is  $10 \text{ mV s}^{-1}$  in all experiments. The pH of the solution was adjusted by  $\text{H}_2\text{SO}_4$  or  $\text{NaOH}$ .

electrochemically active electrode under the neutral or alkaline conditions.

The electrochemistry of oxygen reduction reaction (ORR) has been well established.<sup>36, 37</sup> Redox reactions and the corresponding redox potentials of oxygen under acidic and alkaline conditions are expressed, respectively, as Equations 1 and 2.



According to the data presented in Fig. 2a, the redox potential of  $MV^{2+}/MV^+$  under a neutral or an alkaline condition is *ca.* -0.4 V (vs. SHE). Therefore, if an MV - air cell is operated under the traditional principle with the same alkaline or neutral electrolyte at both the anode and cathode, the theoretical voltage of the resulting cell will be 0.8 V. The cell voltage will be even lower under the practical cell working conditions at higher current densities. Such a low voltage makes the MV-air cell unable to meet the practical application demand as an electrochemical energy storage system.

However, if the MV-air cell is operated with a neutral or alkaline MV anode and an acidic air cathode, a reasonably high theoretical cell voltage (*ca.* 1.6 V) can be achieved. Unfortunately, under the conventional cell operation principle by employing a porous separator, it would not allow developing such a dual-electrolyte cell. The acidic cathode electrolyte and the neutral anode electrolyte would mix with each other during cell operation. Herein, we strategically operate the MV-air cell with an acidic cathode electrolyte (catholyte) and a neutral anode electrolyte (anolyte). The catholyte and anolyte with different pH values are physically and electrically separated with a sodium-ion ( $\text{Na}^+$ -ion) conductive solid-state electrolyte (Na-SSE) membrane, as schematized in Fig. 3. The redox reactions at the acidic air cathode and the neutral MV anode are sustained by the migration of  $\text{Na}^+$ -ions as an ionic messenger through the Na-SSE. To minimize the overpotential of the oxygen redox reaction at the positive electrode, a decoupled positive electrode configuration was applied to the MV-air cell by employing a Ti supported  $\text{IrO}_2$  ( $\text{IrO}_2/\text{Ti}$ ) catalyst for the oxygen evolution reaction (OER) and a Pt/C (carbon supported platinum) catalyst for the oxygen reduction reaction (ORR). The as such fabricated cell is termed as MV (neutral) || Na-SSE || air (acid).

During the charge of an MV (neutral) || Na-SSE || air (acid) cell,  $\text{H}_2\text{O}$  is oxidized to  $\text{O}_2$  on the  $\text{IrO}_2/\text{Ti}$  OER catalyst. This process releases four electrons to the external circuit and releases four protons into the catholyte. At the anode, the  $[(\text{C}_6\text{H}_7\text{N})_2]\text{Cl}_2$  ( $MV^{2+}$ ) is reduced to  $[(\text{C}_6\text{H}_7\text{N})_2]\text{Cl}$  ( $MV^+$ ) by obtaining electrons via the external circuit. This process also releases a  $\text{Cl}^-$  ion in the anolyte. In order to balance the ionic charge transfer between the catholyte and anolyte, sodium ions migrate via the Na-SSE from the cathode electrolyte to the anode electrolyte and couple with the released  $\text{Cl}^-$  ions. During the discharge process, the reactions are reversed. At the anode, the  $[(\text{C}_6\text{H}_7\text{N})_2]\text{Cl}$  ( $MV^+$ ) is oxidized to  $[(\text{C}_6\text{H}_7\text{N})_2]\text{Cl}_2$  ( $MV^{2+}$ ) by combining with the  $\text{Cl}^-$  ions and releasing one electron to the external circuit while the  $\text{Na}^+$ -ions diffuse back to the cathode electrolyte through the Na-SSE. At the cathode, the  $\text{O}_2$  is reduced to water on the Pt/C ORR catalyst by receiving electrons from the external circuit.

The electrochemical kinetics of the  $MV^{2+}/MV^+$  redox reaction was further studied with CV experiments. Fig. 4a shows the CV profiles of the platinum electrode in a solution

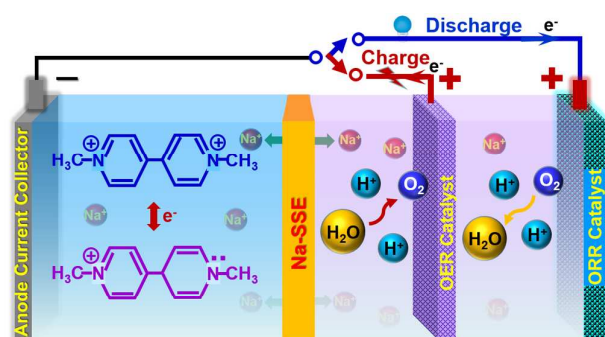


**Fig. 3.** Schematic of a methyl viologen-air cell with an acidic catholyte, a neutral anolyte, and a sodium-ion conductive solid electrolyte membrane. The cell is operated with a decoupled configuration for the air cathode. A Pt/C catalyst is used for the oxygen reduction reaction (ORR) and an IrO<sub>2</sub>/Ti catalyst is used for the oxygen evolution reaction (OER).

containing 0.1 M [(C<sub>6</sub>H<sub>7</sub>N)<sub>2</sub>]Cl<sub>2</sub> and 0.5 M Na<sub>2</sub>SO<sub>4</sub> at different scan rates. At each scan rate, the electrochemical process of the MV<sup>2+</sup>/MV<sup>+</sup> is perfectly reversible. Peak current densities ( $I_{peak}$ ) as a function of the square root of scan rate ( $V^{1/2}$ ) for the cathodic (MV<sup>2+</sup> → MV<sup>+</sup>) and the anodic (MV<sup>+</sup> → MV<sup>2+</sup>) reactions are, respectively, summarized in Figs. 4b and c. The data were derived from Fig. 4a. In both the cathodic and the anodic cases, the  $I_{peak}$  vs.  $V^{1/2}$  shows a perfect linear relationship. This implies that either the reduction of MV<sup>2+</sup> or the oxidation of MV<sup>+</sup> is a mass-transport control process. Therefore, the diffusion coefficients of MV<sup>2+</sup> and MV<sup>+</sup> species can be calculated according to the Randles-Sevcik equation.<sup>38, 39</sup>

$$I_p = 269000 * S * D^{1/2} * n^{3/2} * v^{1/2} * C \quad (3)$$

where  $I_p$  is the peak current density (in A cm<sup>-2</sup>),  $S$  represents the area of the electrode (in cm<sup>2</sup>),  $D$  refers to the diffusion coefficient of the electrochemically active species (in cm<sup>2</sup> s<sup>-1</sup>),  $n$  is the number of electrons transferred in the electrochemical reaction,  $v$  is the

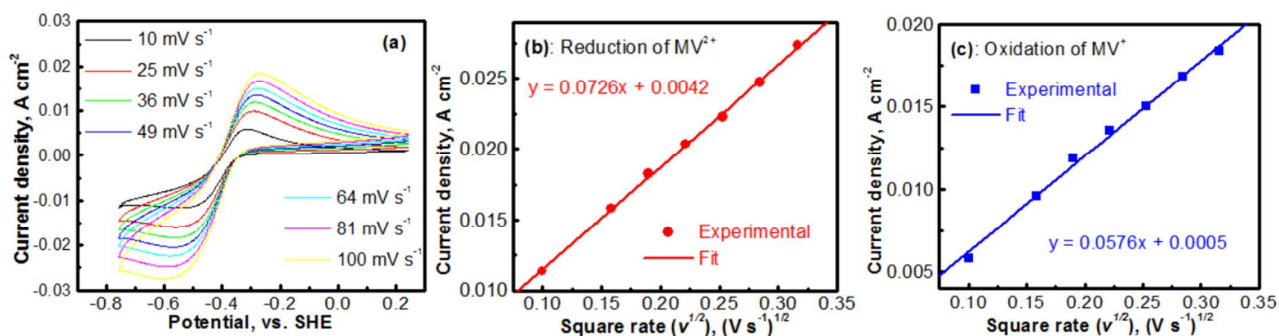


**Fig. 4.** (a) Cyclic Voltammograms (CVs) of the platinum electrode in a 0.1 M [(C<sub>6</sub>H<sub>7</sub>N)<sub>2</sub>]Cl<sub>2</sub> + 0.5 M Na<sub>2</sub>SO<sub>4</sub> solution at different scan rates. (b) Current density as a function of square root of the scan rate (Randles–Sevcik plot) for the [(C<sub>6</sub>H<sub>7</sub>N)<sub>2</sub>]Cl<sub>2</sub> reduction reaction. (c) Randles–Sevcik plot for the [(C<sub>6</sub>H<sub>7</sub>N)<sub>2</sub>]Cl oxidation reaction.

scan rate (in V s<sup>-1</sup>) of the CV experiments, and  $C$  represents the concentration of the redox species (in mol mL<sup>-3</sup>). According to the slope values of the linear plots in Fig. 4b and c, the diffusion coefficient for the reduction of MV<sup>2+</sup> and that for the oxidation of MV<sup>+</sup> can be calculated based on Eq. 3. The  $D$  values of the reduction of MV<sup>2+</sup> and the oxidation of MV<sup>+</sup> are, respectively,  $7.28 \times 10^{-6}$  and  $4.59 \times 10^{-6}$  cm<sup>2</sup> s<sup>-1</sup>. The diffusion coefficients calculated with the experimental data here are basically consistent with those in previous reports.<sup>40, 41</sup>

The sodium mediator-ion SSE employed in this study is a NASICON-type material with a composition of Na<sub>3</sub>Zr<sub>2</sub>Si<sub>2</sub>PO<sub>12</sub>. This material exhibits a sodium-ion conductivity of ca.  $1.0 \times 10^{-3}$  S. cm<sup>-1</sup> at room temperature.<sup>42</sup> To ensure a high surface area for accommodating the liquid MV<sup>2+</sup> and MV<sup>+</sup> active electrode materials, a piece of carbon cloth purchased from the Fuel Cell Store was used as the anode matrix. A picture and a scanning electron microscope (SEM) image showing the high surface fabric of the carbon cloth are provided in Fig. S1. The IrO<sub>2</sub>/Ti OER catalyst was prepared by depositing a thin layer of IrO<sub>2</sub> on the surface of Ti mesh as described in the experimental procedure of the Electronic Supplementary Information (ESI). A picture, as well as an SEM image of the IrO<sub>2</sub>/Ti OER catalyst, are provided in Fig. S2.

The anolyte of this study was prepared with 0.1 M [(C<sub>6</sub>H<sub>7</sub>N)<sub>2</sub>]Cl<sub>2</sub> + 0.5 M Na<sub>2</sub>SO<sub>4</sub>. Therefore, the MV (neutral) || Na-SSE || air (acid) cell was actually assembled in the discharge state. It should be noted that toward practical applications, high-concentration anolyte would be preferred in order to achieve a high energy density with the cell. However, in this proof-of-concept study, the cell was operated with a relatively low-concentration anolyte to avoid any solubility limitation problems. Effects of the concentration of anolyte on the cell performances will be systematically studied in the future. Fig. 5a shows the initial charge profile of the MV (neutral) || Na-SSE || air (acid) cell. In order to avoid the formation of insoluble MV<sup>0</sup>, the cell was charged to a depth of 80% on the basis of the theoretical capacity of the MV<sup>2+</sup>/MV<sup>+</sup> redox couple. Therefore, there does not appear a rising point in the first charge profile in Fig. 5a. To confirm the transition of MV<sup>2+</sup> to MV<sup>+</sup>, the charge product of the anolyte was analyzed with ultraviolet-visible spectroscopy (UV-Vis). Fig. 5b shows the UV-Vis spectra of the fresh [(C<sub>6</sub>H<sub>7</sub>N)<sub>2</sub>]Cl<sub>2</sub> anolyte and after being

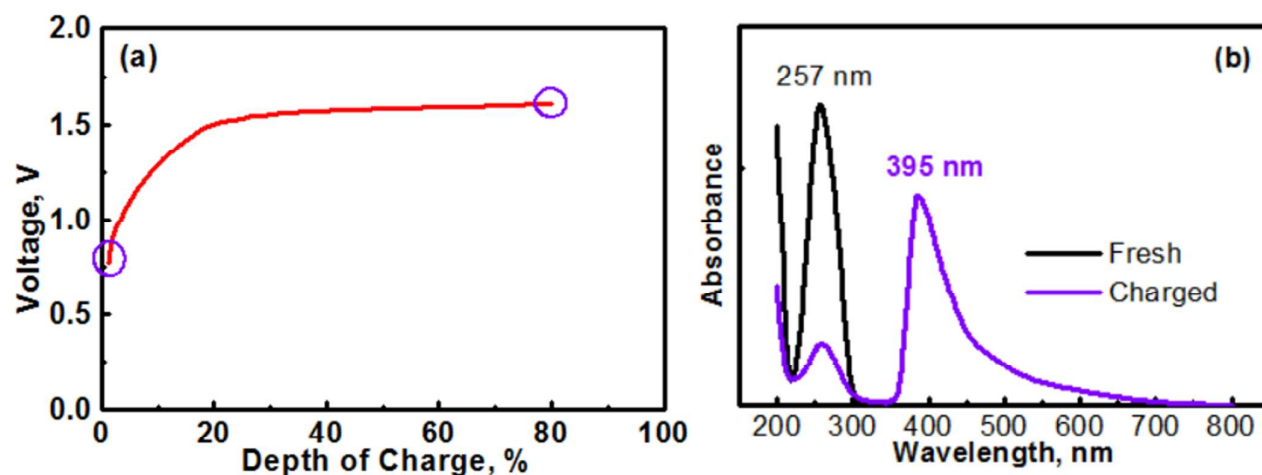


**Fig. 5.** (a) A charge profile of the MV (neutral) || Na-SSE || air (acid) cell. (b) UV-Vis (ultraviolet-visible) spectra of the fresh  $[(C_6H_7N)_2]Cl_2$  anolyte and the anolyte after charging the cell to a depth of 80%, as marked with the purple circles in the charge profile in Fig. 5a.

charged to a depth of 80%, as indicated by the purple circles in Fig. 5a. The absorption peaks located at 257 nm is attributed to the  $MV^{2+}$  species.<sup>43, 44</sup> The appearance of an absorption peak at 395 nm in the spectrum of the charged anolyte indicates the formation of  $MV^+$ .<sup>43</sup> The absorbance of the  $MV^{2+}$  peak for the charged anolyte is *ca.* 22% of that for the fresh  $[(C_6H_7N)_2]Cl_2$  anolyte, indicating *ca.* 78% of the  $MV^{2+}$  species has been reduced to the  $MV^+$ . This result is consistent with the assigned depth of charge of the MV (neutral) || Na-SSE || air (acid) cell. The transition of  $MV^{2+}$  to  $MV^+$  can also be visually observed since there is a color change upon the reduction of the  $MV^{2+}$  species.<sup>45, 46</sup> Fig. S3 presents the color change of the anolyte during charging an MV (neutral) || Na-SSE || air (acid) cell. For the convenience of observation, the anolyte chamber was specially designed with a crescent-shape groove in the lower right corner and a piece of Ti mesh (rather than the high-surface carbon cloth) was used as the anode current collector. As seen in Fig. S3, the fresh anolyte is colorless

before charging. After the cell was charged for 1 h at a current density of  $1.0 \text{ mA cm}^{-2}$ , the anolyte exhibits a violet color. After charging for 2 h, the color of anolyte became even darker.

Fig. 6 presents the cycling performances of the MV (neutral) || Na-SSE || air (acid) cell. The cell was operated with a separate OER electrode and ORR electrode, as described in the experimental section of ESI. The charge and discharge profiles were individually recorded with two separate channels on a battery testing instrument. A 5-minute resting time was preset between each charge and discharge period. Fig. 6a presents the voltage polarization curves of the MV (neutral) || Na-SSE || air (acid) cell. Upon applying a charge-discharge current, the cell voltage responds accordingly. As seen in Fig. 6a, the charge voltage of the cell increases and the discharge voltage decreases with the increase in the cycling current. The high polarization behavior of the cell is mostly due to the relatively low  $Na^+$ -ion conductivity of the Na-SSE and the relatively high thickness (*ca.* 0.7 mm) of the Na-SSE membrane used for the fabrication of the cell. Reducing the

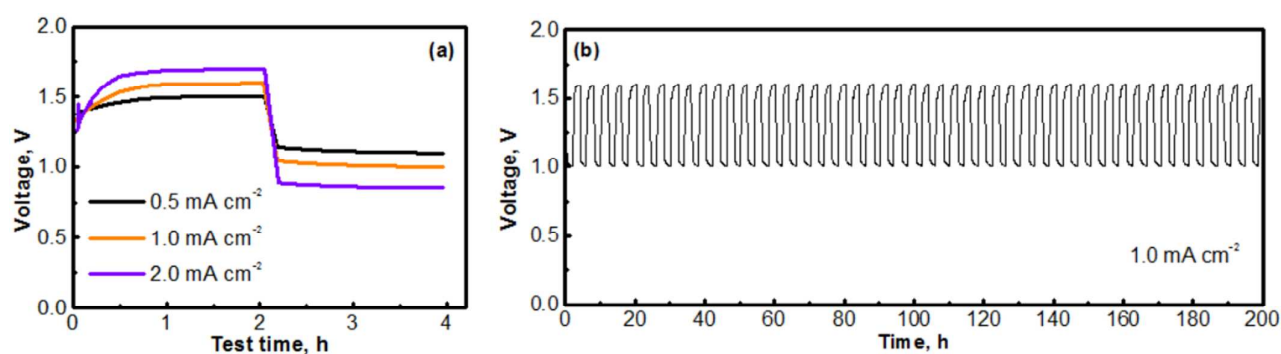


**Fig. 6.** (a) Voltage polarization curves of the MV (neutral) || Na-SSE || air (acid) cells at different operating current densities. (b) Consecutive charge-discharge curves of the MV (neutral) || Na-SSE || air (acid) cell cycled at  $1.0 \text{ mA cm}^{-2}$ .

thickness of the Na-SSE pellet with proper techniques is underway in our lab. Upon being able to fabricate a thin SSE membrane, the MV (neutral) || Na-SSE || air (acid) cell will be able to be cycled at high current densities. Fig. 6b shows the consecutive charge-discharge profile of the MV (neutral) || Na-SSE || air (acid) cell at a cycling current density of 1.0 mA cm<sup>-2</sup>. The consecutive charge-discharge curves of the cell operated at other current densities are provided in Fig. S4. As seen in Fig. 6b and Fig. S4, the cycling profiles show consistent charge and discharge voltages throughout the 50 cycles. There does not appear to be significant changes in the voltage polarization with a continuous cycling of the cell. Fig. S5 shows an SEM image of a cycled (after 50 cycles) carbon cloth matrix. In comparison to the fresh electrode (Fig. S1), there is no obvious change observed in terms of the integrity of the carbon fiber. The stable cycling performance also indicates that different liquid electrolytes at the anode and the cathode are completely separated by the Na-SSE and the electrochemical reactions at the two electrodes are effectively mediated by the shuttling of the sodium ions.

## Conclusions

In summary, this study has demonstrated an electrochemical energy storage system with a novel methyl viologen-air (O<sub>2</sub>) chemistry that is enabled by a mediator-ion solid electrolyte strategy. Operation of the cell with an acidic cathode electrolyte (catholyte) and a neutral anode electrolyte (anolyte) offers a reasonable cell voltage. Under the mediator-ion operating principle, the neutral anolyte and the acidic catholyte are electrically and physically separated by a Na<sup>+</sup>-ion conductive solid-state electrolyte (Na-SSE) membrane. The sodium ions shuttling through the solid-state electrolyte act as ionic mediator to maintain the ionic charge balance between the two electrodes and to maintain the redox reactions at the cathode and anode.

## Conflicts of interest

There are no conflicts of interest to declare.

## Acknowledgments

This work was supported by the U.S. Department of Energy, Office of Basic Energy Sciences, Division of Materials Sciences and Engineering under award number DE-SC0005397.

## Notes and references

- G. L. Soloveichik, *Chem Rev*, 2015, **115**, 11533-11558.
- L. J. Li and A. Manthiram, *Adv Energy Mater*, 2016, **6**, 1502054.
- A. Manthiram, Yu, X., Wang, S., *Nat Rev Mater*, 2017, **2**, 16103.
- P. Alotto, M. Guarnieri and F. Moro, *Renew Sust Energy Rev*, 2014, **29**, 325-335.
- X. W. Yu, M. M. Gross, S. F. Wang and A. Manthiram, *Adv Energy Mater*, 2017, **7**, 1602454.
- J. Winsberg, T. Hagemann, T. Janoschka, M. D. Hager and U. S. Schubert, *Angew Chem Int Edit*, 2017, **56**, 686-711.
- X. L. Wei, W. X. Pan, W. T. Duan, A. Hollas, Z. Yang, B. Li, Z. M. Nie, J. Liu, D. Reed, W. Wang and V. Sprenkle, *ACS Energy Letters*, 2017, **2**, 2187-2204.
- M. Park, J. Ryu, W. Wang and J. Cho, *Nat Rev Mater*, 2017, **2**, 16080.
- C. M. Araujo, D. L. Simone, S. J. Konezny, A. Shim, R. H. Crabtree, G. L. Soloveichik and V. S. Batista, *Energ Environ Sci*, 2012, **5**, 9534-9542.
- C. S. Sevov, R. E. M. Brooner, E. Chenard, R. S. Assary, J. S. Moore, J. Rodriguez-Lopez and M. S. Sanford, *J Am Chem Soc*, 2015, **137**, 14465-14472.
- X. W. Yu and A. Manthiram, *Joule*, 2017, **1**, 453-462.
- B. Huskinson, M. P. Marshak, C. Suh, S. Er, M. R. Gerhardt, C. J. Galvin, X. D. Chen, A. Aspuru-Guzik, R. G. Gordon and M. J. Aziz, *Nature*, 2014, **505**, 195-198.
- T. Janoschka, N. Martin, U. Martin, C. Friebe, S. Morgenstern, H. Hiller, M. D. Hager and U. S. Schubert, *Nature*, 2015, **527**, 78-81.
- B. Hu, C. DeBruler, Z. Rhodes and T. L. Liu, *J Am Chem Soc*, 2017, **139**, 1207-1214.
- W. Wang and V. Sprenkle, *Nat Chem*, 2016, **8**, 204-206.
- A. C. Luntz and B. D. McCloskey, *Chem Rev*, 2014, **114**, 11721-11750.
- Y. G. Li and H. J. Dai, *Chem Soc Rev*, 2014, **43**, 5257-5275.
- P. Gu, M. B. Zheng, Q. X. Zhao, X. Xiao, H. G. Xue and H. Pang, *J Mater Chem A*, 2017, **5**, 7651-7666.
- Y. G. Li and J. Lu, *Acs Energy Letters*, 2017, **2**, 1370-1377.
- L. J. Li and A. Manthiram, *Nano Energy*, 2014, **9**, 94-100.
- L. J. Li, S. H. Chai, S. Dai and A. Manthiram, *Energ Environ Sci*, 2014, **7**, 2630-2636.
- N. Imanishi and O. Yamamoto, *Mater Today*, 2014, **17**, 24-30.
- J. Fu, Z. P. Cano, M. G. Park, A. P. Yu, M. Fowler and Z. W. Chen, *Adv Mater*, 2017, **29**, 1604685.
- Z. Ma, X. X. Yuan, L. Li, Z. F. Ma, D. P. Wilkinson, L. Zhang and J. J. Zhang, *Energ Environ Sci*, 2015, **8**, 2144-2198.
- D. Zhang, C. Z. Zhang, D. B. Mu, B. R. Wu and F. Wu, *Prog Chem*, 2012, **24**, 2472-2482.
- Y. Ding and G. H. Yu, *Angew Chem Int Edit*, 2017, **56**, 8614-8616.
- B. Hu, C. Seefeldt, C. DeBruler and T. L. Liu, *J Mater Chem A*, 2017, **5**, 22137-22145.
- I. Shpilevaya and J. S. Foord, *Electroanal*, 2014, **26**, 2088-2099.
- J. R. White and A. J. Bard, *J Electroanal Chem*, 1986, **197**, 233-244.
- P. M. S. Monk, R. D. Fairweather, M. D. Ingram and J. A. Duffy, *J Chem Soc Perk T 2*, 1992, 2039-2042.
- A. Walcarius, L. Lamberts and E. G. Derouane, *Electroanal*, 1995, **7**, 120-128.
- O. Enea, *Electrochim Acta*, 1986, **31**, 789-793.
- T. W. Hui and M. D. Baker, *J Phys Chem B*, 2002, **106**, 827-832.
- I. Okura, S. Nakamura, N. Kimthuan and K. I. Nakamura, *J Mol Catal*, 1979, **6**, 261-267.
- C. L. Bird and A. T. Kuhn, *Chem Soc Rev*, 1981, **10**, 49-82.
- H. Y. Yuan, Y. Hou, I. M. Abu-Reesh, J. H. Chen and Z. He, *Mater Horiz*, 2016, **3**, 382-401.
- T. J. Schmidt, V. Stamenkovic, P. N. Ross and N. M. Markovic, *Phys Chem Chem Phys*, 2003, **5**, 400-406.

## ARTICLE

## Journal Name

38. C. M. A. Brett and A. M. O. Brett, *Electrochemistry Principles, Methods and Applications*, Oxford University Press, Oxford/New York, 1993.
39. M. C. Henstridge, E. Laborda, E. J. F. Dickinson and R. G. Compton, *J Electroanal Chem*, 2012, **664**, 73-79.
40. Q. Q. Lin, Q. Li, C. Batchelor-McAuley and R. G. Compton, *J Electrochem Sci Te*, 2013, **4**, 71-80.
41. R. A. Mackay, S. A. Myers and A. BrajterToth, *Electroanal*, 1996, **8**, 759-764.
42. J. K. Kim, E. Lee, H. Kim, C. Johnson, J. Cho and Y. Kim, *Chemelectrochem*, 2015, **2**, 328-332.
43. J. F. Stargardt and F. M. Hawkridge, *Anal Chim Acta*, 1983, **146**, 1-8.
44. J. Peon, X. Tan, J. D. Hoerner, C. G. Xia, Y. F. Luk and B. Kohler, *J Phys Chem A*, 2001, **105**, 5768-5777.
45. D. Wang, W. E. Crowe, R. M. Strongin and M. Sibrian-Vazquez, *Chem Commun*, 2009, 1876-1878.
46. Y. S. Park, S. Y. Um and K. B. Yoon, *J Am Chem Soc*, 1999, **121**, 3193-3200.

## A Strategically Managed Rechargeable Battery System with a Neutral Methyl Viologen Anolyte and an Acidic Air-Cathode Enabled by a Mediator-ion Solid Electrolyte

Xingwen Yu and Arumugam Manthiram\*

A “mediator-ion” solid-electrolyte membrane strategy enables the operation of methyl viologen – air batteries with a neutral anolyte and an acidic catholyte.

